

REPORT DOCUMENTATION PAGE

AFRL-SR-AR-TR-04-

Public reporting burden for this collection of information is estimated to average 1 hour per response, including the time for reviewing the data needed, and completing and reviewing this collection of information. Send comments regarding this burden suggestions for reducing this burden to Washington Headquarters Services, Directorate for Information Operations and Reports, and to the Office of Management and Budget, Paperwork Reduction Project (0704-0188), Washington, DC 20503

0479

1. AGENCY USE ONLY (Leave blank)		2. REPORT DATE 1 Sep 2004		3. REPORT TYPE AND Final Report, 1 Sep 2002 - 1 Sep 2003	
4. TITLE AND SUBTITLE DEVELOPMENT AND APPLICATION OF ADVANCED ALGORITHMS FOR THE SIMULATION OF VISCOUS COMPRESSIBLE FLOWS WITH MOVING BODIES IN THREE DIMENSIONS				5. FUNDING NUMBERS G F49620-03-1-0071	
6. AUTHOR(S) Rainald Lohner and Chi Yang					
7. PERFORMING ORGANIZATION NAME(S) AND ADDRESS(ES) George Mason University MS 4C7, SCS 4400 University Drive Fairfax, VA 22033				8. PERFORMING ORGANIZATION REPORT NUMBER 5-25024	
9. SPONSORING / MONITORING AGENCY NAME(S) AND ADDRESS(ES) Air Force Office of Scientific Research Bolling Air Force Base Dr. Leonidas Sakell Washington, D.C. 20332-6448				10. SPONSORING / MONITORING AGENCY REPORT NUMBER	
11. SUPPLEMENTARY NOTES					
12a. DISTRIBUTION / AVAILABILITY STATEMENT No limitation				12b. DISTRIBUTION CODE	
13. ABSTRACT (Maximum 200 Words) The overall objective of the research carried out last year was the development of new algorithms for the efficient simulation of viscous compressible flows with moving bodies in three dimensions. The development was based on current 3-D Euler/Navier-Stokes capabilities, and encompassed flow solvers, grid generation, adaptive embedded unstructured grid methods, optimal shape design, and the efficient use of emerging super computer hardware. The research carried out over last years significantly advanced the state of the art in this area of CFD.					
DISTRIBUTION STATEMENT A Approved for Public Release Distribution Unlimited					
14. SUBJECT TERMS CFD, embedded unstructured grids, optimal shape design				15. NUMBER OF PAGES 12	
				16. PRICE CODE	
17. SECURITY CLASSIFICATION OF REPORT	18. SECURITY CLASSIFICATION OF THIS PAGE	19. SECURITY CLASSIFICATION OF ABSTRACT		20. LIMITATION OF ABSTRACT	

NSN 7540-01-280-5500

BEST AVAILABLE COPY

Standard Form 298 (Rev. 2-89)
Prescribed by ANSI Std. Z39-18
298-102

20040922 009

FINAL REPORT: DECEMBER 2003

DEVELOPMENT AND APPLICATION OF ADVANCED ALGORITHMS FOR
THE SIMULATION OF VISCOUS COMPRESSIBLE FLOWS
WITH MOVING BODIES IN THREE DIMENSIONS

Rainald Löhner and Chi Yang
School of Computational Sciences
George Mason University
Fairfax, VA 22030-4444

presented to:

Air Force Office of Scientific Research /NA
c/o Dr. Leonidas Sakell
Bolling Air Force Base
Washington, D.C. 20332-6448

FINAL REPORT: DECEMBER 2003

DEVELOPMENT AND APPLICATION OF ADVANCED ALGORITHMS FOR THE SIMULATION OF VISCOUS COMPRESSIBLE FLOWS WITH MOVING BODIES IN THREE DIMENSIONS

Rainald Löhner and Chi Yang
School of Computational Sciences
George Mason University
Fairfax, VA 22030-4444

Summary

The overall objective of the research carried out over last year was the development of new algorithms for the efficient simulation of viscous compressible flows with moving structurally and thermally responding bodies in three dimensions using unstructured grids. The development was based on current 3-D Euler/Navier-Stokes capabilities, and encompassed:

- Grid Generation;
- Flow Solvers;
- Adaptive embedded unstructured grid methods;
- Optimal shape design.

These topics are treated below in some more detail.

1. GRID GENERATION

Many simulation techniques in computational mechanics require a space-filling cloud of arbitrary objects. For the case of 'gridless' or 'mesh free' partial differential equation (PDE) solvers, these are simply points. For discrete element methods these could be spheres, ellipsoids, polyhedra, or any other arbitrary shape. The task is therefore to fill a prescribed volume with these objects so that they are close but do not overlap in an automatic way.

Several techniques have been used to place these objects in space. The so-called 'fill and expand' or 'popcorn' technique starts by first generating a coarse mesh for the volume to be filled. This subdivision of the volume into large, simple polyhedra (elements), is, in most cases performed with hexahedra. The objects required (points, spheres, ellipsoids, polyhedra, etc.) are then placed randomly in each of these elements. These are then expanded in size until contact occurs or the desired fill-ratio has been achieved. An obvious drawback of this technique is the requirement of a mesh generator to initiate the process. A second class of techniques are the 'advancing front' or 'depositional'

methods. Starting from the surface, objects are added where empty space still exists. In contrast to the 'fill and expand' procedures, the objects are packed as close as required during introduction. Depending on how the objects are introduced, one can mimic gravitational or magnetic deposition, layer growing, or size-based growth. Furthermore, so-called radius growing can be achieved by first generating a coarse cloud of objects, and then growing more objects around each of these. In this way, one can simulate granules or stone.

We developed a scheme that allows for the direct generation of clouds of arbitrary objects with the same degree of flexibility as advanced unstructured mesh generators. The mean distance between objects (or, equivalently, the material density) is specified by means of background grids, sources and density attached to CAD-entities. In order not to generate objects outside the computational domain, we assume an initial triangulation of the surface that is compatible with the desired mean distance between objects specified by the user. Starting from this initial 'front' of objects, new objects are added, until no further objects can be introduced. Whereas the advancing front technique for the generation of volume grids removes one face at a time to generate elements, the present scheme removes one object at a time, attempting to introduce as many objects as possible in its immediate neighbourhood.

2. FLOW SOLVERS

Any coupled fluid-structure capability requires an advanced, robust flow solver that works optimally across the range of physical phenomena and associated spatial and temporal scales. We have made improvements on simulating three-dimensional compressible turbulent flows for complex geometries.

Computational fluid dynamics (CFD) has become an indispensable tool for the aerodynamic design and analysis of aircrafts and engines. The difficulty of generating structured grids and the desire to compute flows over increasingly complex configurations has fueled interest in the development of unstructured grid methods. Unstructured grids provide great flexibility in tackling complex geometries encountered in practice and offer a natural framework for adapting to flow features. Nowadays, unstructured grids composed of geometric simplices, i.e., triangle in two dimensions and tetrahedra in three dimensions are widely and routinely used for producing high-quality solutions for both inviscid flows and low Reynolds number viscous flows. However, so far, the solution of the Navier-Stokes equations for high Reynolds number viscous flows has been dominated by structured grid methods, as grid stretching along shear layers is a trivial task on structured meshes but is relatively difficult to achieve on unstructured triangular or tetrahedral grids. One popular approach has been to use a hybrid grid: prismatic elements are used for viscous regions where the grid is highly stretched, and tetrahedral elements for inviscid regions where the grid is nearly isotropic. Although this approach seems to be attractive, the need to generate a prismatic grid unavoidably renders the grid generation more difficult and less robust for complex geometries, which would otherwise has been the main advantage of unstructured grid methods. In fact,

one can easily show that the prismatic grid generator will fail for the corners, where the newly created point is not visible from all the faces surrounding the original point. Furthermore, the existence of several cell types in a hybrid grid undoubtedly makes mesh generation and adaptation, flow solution, and post-processing more complex.

We have developed a parallel, accurate, fast, matrix-free implicit method to solve compressible turbulent flow problems using the Spalart and Allmaras one equation turbulence model on unstructured meshes. In this method, the mean-flow and turbulence-model equations are decoupled in the time integration in order to facilitate the incorporation of different turbulence models and reduce memory requirements. Both mean flow and turbulent equations are integrated in time using a linearized implicit scheme. A fast, matrix-free implicit method, GMRES+LU-SGS, is then applied to solve the resultant system of linear equations. The spatial discretization is carried out using a hybrid finite volume and finite element method, where the finite volume approximation based on a containment dual control volume rather than on the more popular median-dual control volume is used to discretize the inviscid fluxes, and the finite element approximation is used to evaluate the viscous flux terms.

The developed method has been used to compute a variety of compressible turbulent flow problems over a wide range of flow conditions. The computational results demonstrated that this unstructured tetrahedral grid method is able to produce same quality solutions as its hybrid counterpart.

The developed method has been used to predict drags in the transonic regime for both DLR-F4 and DLR-F6 configurations to assess the accuracy and efficiency of the method. The results obtained are in good agreement with experimental data, indicating that the present method provides an accurate, efficient, and robust algorithm for computing turbulent flows for complex geometries on unstructured grids.

3. ADAPTIVE EMBEDDED UNSTRUCTURED GRID METHODS

The numerical solution of Partial Differential Equations (PDEs) is usually accomplished by performing a spatial and temporal discretization with subsequent solution of a large algebraic system of equations. The spatial discretization is commonly performed via polyhedra, also called (finite) volumes or elements. The final assembly of these polyhedra yields the so-called mesh. The transition from an arbitrary surface description to a proper mesh still represents a difficult task. Considering the rapid advance of computer power, together with the perceived maturity of field solvers, an automatic transition from arbitrary (and possibly imperfect or dirty) surface description to mesh becomes mandatory.

Two types of grids are most commonly used: body-conforming and embedded. For body-conforming grids the external mesh faces match up with the surface (body surfaces, external surfaces, etc.) of the domain. This is not the case for the embedded approach (also known as fictitious domain, immersed boundary or Cartesian method), where the surface is placed inside a large mesh (typically a regular parallelepiped), with special treatment of the elements close to the surfaces.

Prompted by the need to solve shock-structure interaction problems and the inability of Computational Structural Dynamics (CSD) codes to ensure strict no-penetration during contact, a simple embedded technique operating on adaptive, unstructured grids was developed in FY 2003. The essential elements of this technique may be summarized as follows:

- a) The key modification of the original, body fitted edge-based solver was the removal of all geometry-parameters (essentially the area normals) belonging to edges cut by embedded surface faces.
- b) Several techniques to improve the treatment of boundary points close to the immersed surfaces were implemented. Higher-order boundary conditions were also achieved by duplicating crossed edges and their endpoints.
- c) Geometric resolution and solution accuracy were enhanced by adaptive mesh refinement that was based on the proximity to or the curvature of the embedded CSD surfaces.
- d) In order to save work, user-defined or automatic deactivation for regions inside immersed solid bodies was employed.

The technique has been extremely successful for complex fluid-structure interaction cases, as well as some external aerodynamics cases. Led on by this success, the technique has seen extensive use, leading to new developments. These developments may be grouped as follows:

- Improvements in **speed**, with particular emphasis on bin data structures;
- Treatment of **multimaterial problems**, in particular water/air;
- **Particle** transport and embedded surfaces;
- Direct link to **Discrete Particle Methods (DPM)**;
- Body-fitted **grid generation** via the embedded approach; and
- Links to simplified **CSD models**.

4. OPTIMAL SHAPE DESIGN

The availability of accurate, reliable and fast CFD solvers immediately leads to the next stage in simulations: optimal shape design. It is the nature of any technical development that an engineer would not only like to know if a certain device performs as required, but how to improve it. One of the most promising ways of solving the optimization problem is via the so-called adjoint formulation. We have developed a scheme based on the solution of a continuous adjoint problem. The computation of the objective function sensitivities is performed by using only the flow and adjoint solutions on the boundary. This property makes the scheme totally independent of the numerical solvers (flow and adjoint). In addition, the scheme allows the use of incomplete gradients by only taking into account the geometrical sensitivities, and/or the boundary conditions of the adjoint problem. An improved pseudo-shell approach to move the surface to be optimized, and to impose the geometric restrictions was developed and tested. We have incorporated above adjoint solvers into FEFLO.

The new developed adjoint solver was used for an incompressible Navier-Stokes control problem, and a compressible shape design problem. The control problem consists of minimizing the amplitude of the periodic pressure lift force on the cylinder, by moving a portion of the cylinder surface in each time step, or, instead of that, by imposing an equivalent injection velocity. The control starts to be applied at $t = 25$ (500 time steps). The amplitude of the force is reduced by 87% for both types of controls. In addition, it can be noticed that the effect of moving the mesh and of applying the injection velocity is exactly the same. The maximum injection velocity was around 1% of the inflow velocity.

To illustrate how the pseudo-shell approach works, the drag force at constant lift over a hypersonic wing (at an angle of attack of 5°) was optimized, subject to a minimum thickness constraint. It was demonstrated from this numerical example that an improved pseudo-shell approach, to move the objective surface, and to impose general geometric constraints produced smooth shapes in each design cycle.

5. EXAMPLES

The developed unstructured grid solver has applied over the last year to a number of problems. We include here two recent examples in the following section.

5.1 DLR-F4 configuration: The first example considers the test cases for the first AIAA Drag Prediction Workshop held in Anaheim, CA June 2001. The workshop challenge was to compute the lift, drag, and pitching moment for the DLR-F4 wing-body configuration for different sets of conditions. For all cases the free stream Mach number is 0.75, and the Reynolds number is 3 millions. The mandatory calculations for the Drag Prediction Workshop were performed using the standard unstructured nodal grid, which contains 9,650,674 elements, 1,641,451 points, and 48,339 boundary points, as shown in Figure 1a. All computations were initiated as a uniform flow at freestream conditions, and advanced with a CFL number of 200. The relative L_2 norm of the density residual is taken as the criterion for convergence history. The solution tolerance for GMRES was set to 0.1 with 10 search directions and 20 iterations. We observed that during the first few time steps, more iterations are required to solve the system of the linear equations: even 20 iterations can not guarantee that the stopping criterion will be satisfied for some cases. However, it takes less than 20 iterations to solve the linear equations at a later time, and global convergence is not affected by a lack of linear system convergence during the first few time steps. All computations were performed on a SGI origin 2000 (400MHz) computer and required 4 GB memory and about 7 hours on 16 processors for 1000 time-steps. Note that convergence in the lift and drag is obtained in as little as 500 time steps for all cases.

The case with a single point at $C_L=0.5$ is presented here. The computed pressure contours displayed in Fig. 1b, clearly show good resolution of the upper surface shock.

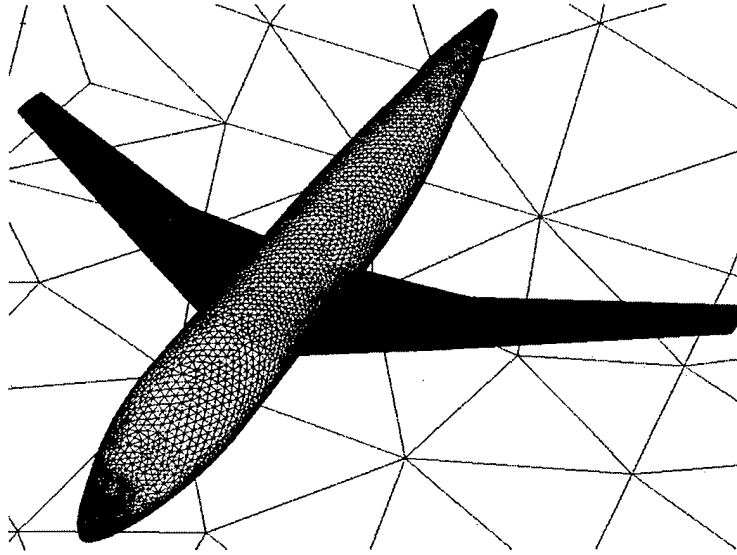


Fig. 1a: Unstructured surface mesh used for computing turbulent flow past DLR-F4 configuration (nelem=9,650,674, npoin=1,641,451, nboun=48,339).

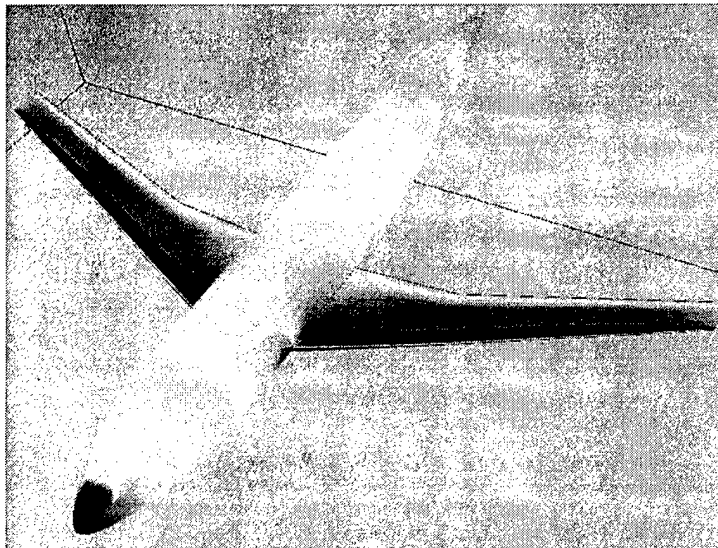


Fig. 1b: Computed pressure contours on the surface of DLR-F4 configuration at $M_\infty = 0.75$, $\alpha = -0.002^\circ$, and $Re=3,000,000$.

Table 1 summarizes the results obtained for case 1 by the experiments, drag prediction workshop participants, and present computation. Although there is a considerable amount of scatter in the data obtained by the drag prediction workshop, our computational results are close to the average data, especially for drag and pitching moment.

Table 1. Comparison of computational results with experimental data and Drag Prediction Workshop data

Data	α	C_L	C_D	C_M
ONERA	0.192	0.50	0.02896	-0.1260
NLR	0.153	0.50	0.02889	-0.1301
DRA	0.179	0.50	0.02793	-0.1371
Workshop(Ave)	-0.237	0.5002	0.03037	-0.1559
Workshop(Min)	-1.000	0.4980	0.02257	-0.2276
Workshop(Max)	1.223	0.5060	0.04998	0.0481
Present	-0.002	0.5009	0.03058	-0.1513

5.2 DLR-F6 configuration: The second example considers the test cases in the 2nd AIAA Drag Prediction Workshop held in Orlando, FL June 2003. The chosen configuration, denoted as DLR-F6, consists of wing-body geometry without or with a conventional nacelle. All computations were performed on the NAVO IBM Cluster 1600 (1.3 GHz Power 4) computer and required less than 8 Gbytes memory and less than 12 hours of CPU on 8 processors. Although the Drag Prediction Workshop specified several mandatory and optional cases, only the mandatory cases were computed in this work. For all cases the free stream Mach number is 0.75, and the Reynolds number based on reference chord of 14.12cm is 3 millions.

The case with a single point at a prescribed lift coefficient of 0.5. is presented here. In order to test the robustness of the present method on grids generated by different grid generators, the grid convergence study was performed using the coarse grid provided by NASA LARC as our coarse grid, the coarse grid provided by Swansea as our medium grid, and the coarse grid by DLR as our fine grid. Table 2 shows the grid size and computed results for the wing-body configuration for case 1 with the three different grids. The comparison of lift and drag coefficients with the experimental data is shown in Figs. 2a-b, respectively. Although there is a considerable amount of scatter in the data obtained by the drag prediction workshop, our computational results are close to the average data. The computed pressure contours on the medium mesh is displayed in Fig. 2c.

Table 2 shows the grid size and computed results for the wing-body-pylon-nacelle configuration with three different grids.

Table 2. Wing/body/pylon/nacelle Configuration

Grid Size	α	C_L	C_D	C_M
1,827,470	0.950	0.497	0.03719	-0.1205
2,419,388	0.843	0.498	0.03658	-0.1216
3,682,535	0.800	0.501	0.03631	-0.1242

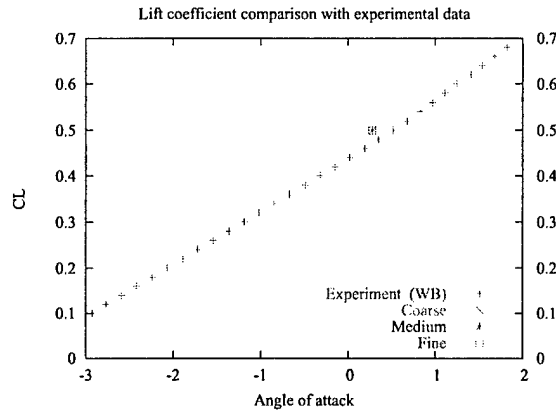


Fig. 2a: Comparison of computed lift coefficient and experimental data for DLR-F6 wing-body configuration at $M_\infty = 0.75$, and $Re=3,000,000$.

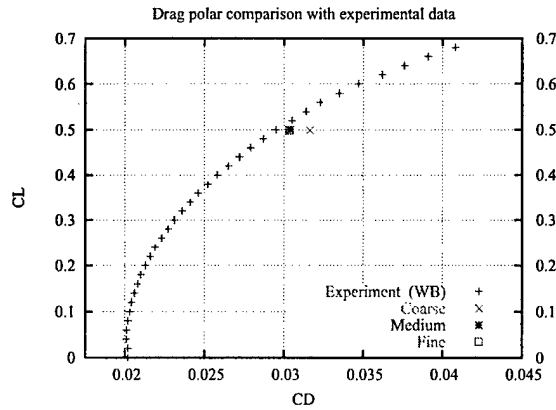


Fig. 2b: Comparison of computed and experimental drag polar for DLR-F6 wing-body configuration at $M_\infty = 0.75$, and $Re=3,000,000$.

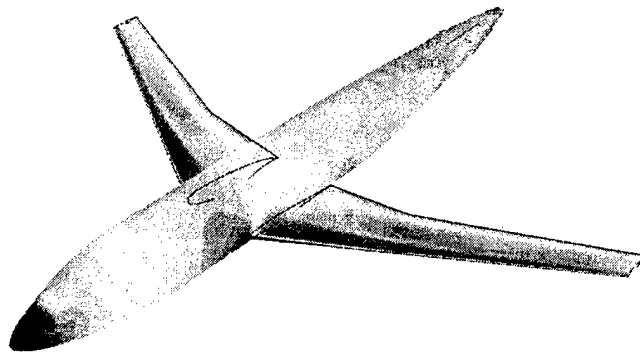


Fig. 2c: Computed pressure contours on the surface of DLR-F6 wing-body configuration at $M_\infty = 0.75$, $C_L=0.5$, and $Re=3,000,000$.

5.3 Design of a 3D wing: The third example considers the minimization of the drag force at constant lift over a hypersonic wing (at an angle of attack of 5°). The wing is subject to a minimum thickness constraint. Figs. 3a shows the Initial geometry and surface mesh on the wing, Fig. 3b shows the initial and final wing geometries after 80 design cycles (the number of design parameters where approximately 3575). The design was mostly dominated by the minimum thickness constraint, even though some small twist and asymmetry were also obtained. The objective function gradients were computed using an incomplete continuous adjoint formulation. The design process was considered finished when the drag and the lift forces did not have any further meaningful variations. The drag improvement was of 60%, which was obtained with a lift increment of 9%.

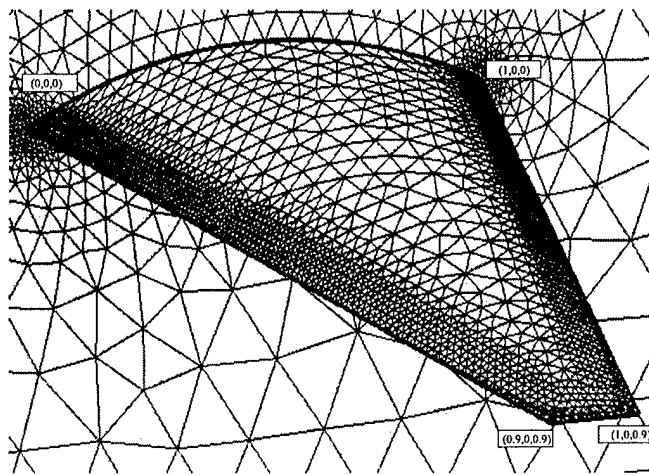


Fig. 3a: Initial geometry and surface mesh on the wing (3575 nodal points). The corner coordinate values are also shown

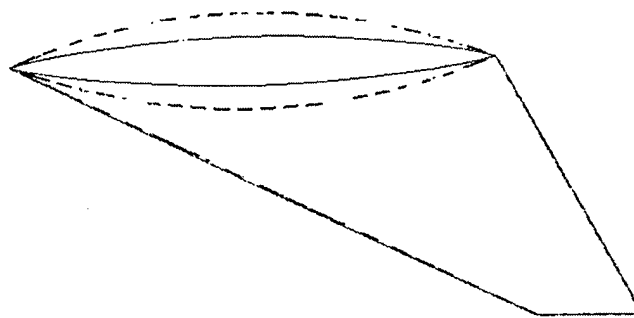


Fig. 3b: Initial (dashed line) and final (continuous line) geometries. A small twist at the final geometry can be noticed.

6. CONCLUSIONS AND OUTLOOK

We developed a scheme that allows for the direct generation of clouds of arbitrary objects with the same degree of flexibility as advanced unstructured mesh generators. We implemented adaptive embedded unstructured grid methods in our flow code. This technique has been extremely successful for complex fluid-structure interaction cases, as well as some external aerodynamics cases. We have developed a new numerical method for computing three-dimensional compressible turbulent flows for complex geometries using a one-equation turbulence model on unstructured grids. The method uses containment dual control volume to discretize the inviscid fluxes to achieve the dramatic improvement in accuracy on a highly stretched tetrahedral mesh and the matrix-free implicit GMRES+LU-SGS method to achieve the fast convergency.

7. REFERENCES

- H. Luo, J.D. Baum and R. Löhner - Computation of Compressible Flows Using a Two-Equation Turbulence Model on Unstructured Grids; *Int. J. CFD* 17, (1), 87-93 (2003).
- O. Soto, R. Löhner and F. Camelli - A Linelet Preconditioner for Incompressible Flows; *Int. J. Num. Meth. Heat and Fluid Flow* 13, (1), 133-147 (2003).
- R. Löhner, J. Cebral, O. Soto, P. Yim and J.E. Burgess - Applications of Patient-Specific CFD in Medicine and Life Sciences; *Int. J. Num. Meth. Fluids* 43, 637-650 (2003).
- D. Sharov, H. Luo, J.D. Baum and R. Löhner - Unstructured Navier-Stokes Grid Generation at Corners and Ridges; *Int. J. Num. Meth. Fluids* 43, 717-728 (2003).
- H. Luo, J.D. Baum and R. Löhner - Parallel Unstructured Grid GMRES+LU-SGS Method for Turbulent Flows; *AIAA-03-0273* (2003).
- H. Luo, J.D. Baum and R. Löhner - Development and Application of Unstructured-Grid Methodologies for Turbulent Flows; *AIAA-03-0277* (2003).
- R. Löhner, O. Soto and Chi Yang - An Adjoint-Based Design Methodology for CFD Optimization Problems; *AIAA-03-0299* (2003).
- F. Camelli, O. Soto, R. Löhner, W. Sandberg and R. Ramamurti - Topside LPD17 Flow and Temperature Study with an Implicit monolithic Scheme; *AIAA-03-0969* (2003).
- R. Löhner, J.D. Baum, E.L. Mestreau, D. Sharov, Ch. Charman and D. Pelessone - Adaptive Embedded Unstructured Grid Methods; *AIAA-03-1116* (2003).
- O. Soto, R. Löhner, J. Cebral and F. Camelli - A Stabilized Edge-Based Implicit Incompressible Flow Solver; *AIAA-03-3836-CP* (2003).

- H. Luo, J.D. Baum, and R. Löhner - Extension of HLLC Scheme for Flows at All Speeds; *AIAA Paper* 2003-3840 (2003).
- R. Löhner, Chi Yang, J.R. Cebal, O. Soto, F. Camelli and J. Waltz - Improving the Speed and Accuracy of Projection-Type Incompressible Flow Solvers; *AIAA-03-3991-CP* [Invited] (2003).
- H. Luo, J.D. Baum and R. Löhner - An ALE Method for Compressible Multi-Material Flows on Unstructured Grids; *AIAA-03-4109* (2003).
- R. Löhner, C. Yang, J. Cebal, O. Soto and F. Camelli - On Incompressible Flow Solvers; pp.50-71 in *Numerical Simulations of Incompressible Flows* (M.M. Hafez ed.), World Scientific (2003).
- R. Löhner, J.D. Baum, Ch. Charman and D. Pelessone - Fluid-Structure Interaction Simulations Using Parallel Computers; pp.3-23 in *VECPAR 2002, LNCS 2565* (J.M.L.M. Palma et al. eds.), Springer Verlag (2003).
- R. Löhner - What Applications Are Realistic in the Next Few Years - A Visionary Outlook; paper presented at the *6th World Fluid Dynamics Days, WUA-CFD*, Nürnberg, Germany, May (2003).
- C. Yang and R. Löhner - Prediction of Flows over an Axisymmetric Body with Appendages, *Proc. of 8th International Conference on Numerical Ship Hydrodynamics*, Busan, Korea, September 22-25 (2003).
- J.R. Cebal, M. Castro, R. Löhner, O. Soto, P.J. Yim and N. Alperin - Realistic Cerebral Circulation Models from Medical Image Data, *Proc. ASME-BED Summer Bioengineering Meeting*, Key Biscayne, FL, June 25-29 (2003).
- R. Löhner and J.D. Baum - 30 Years of FCT: Status and Directions; *Workshop on High Resolution Schemes for Convection-Dominated Flows: 30 Years of FCT*, Dortmund, Germany, September 29-30 (2003).
- R. Löhner - Blast Effects on Structures; *DHS ASC Workshop*, Washington, D.C., October 8-9 (2003).
- J.D. Baum, E. Mestreau, H. Luo, R. Löhner, D. Pelessone and Ch. Charman - Modeling Structural Response to Blast Loading Using a Coupled CFD/CSD Methodology; *Proc. Des. An. Prot. Struct. Impact/ Impulsive/ Shock Loads (DAPSIL)*, Tokyo, Japan, December (2003).